HOKKAIDO UNIVERSITY

Title	Oxygen-17 nuclear magnetic resonance measurements on apatite-type lanthanum silicate (La9.33(SiO4)6O2)
Author(s)	Kiyono, Hajime; Matsuda, Yuuya; Shimada, Toshihiro; Ando, Mariko; Oikawa, Itaru; Maekawa, Hideki; Nakayama, Susumu; Ohki, Shinobu; Tansho, Masataka; Shimizu, Tadashi; Florian, Pierre; Massiot, Dominique
Citation	Solid State Ionics, 228, 64-69 https://doi.org/10.1016/j.ssi.2012.09.016
Issue Date	2012-11
Doc URL	http://hdl.handle.net/2115/51907
Type	article (author version)
File Information	Solid_State_Ionics-228-2012-64_69.pdf

Instructions for use

Oxygen-17 Nuclear Magnetic Resonance Measurements on Apatite-Type Lanthanum Silicate (La$_{9.33}$(SiO$_4$)$_6$O$_2$)

Hajime Kiyono[a*], Yuya Matsuda[b], Toshihiro Shimada[b], Mariko Ando[c], Itaru Oikawa[c], Hideki Maekawa[c], Susumu Nakayama[d], Shinobu Ohki[e], Masataka Tansyo[e], Tadashi Shimizu[e], Pierre Florian[f], and Dominuqie Massiot[f]

[a] *College of Engineering, Shibaura Institute of Technology, 3-7-5, Toyosu, Koto-ku, Tokyo 135-8548, Japan*

[b] *Graduate School of Engineering, Hokkaido University, Kita-ku, Sapporo, Hokkaido, 060-8628 Japan*

[c] *Graduate School of Engineering, Tohoku University, Aoba-ku, Sendai, Miyagi, Japan*

[d] *Department of Applied Chemistry and Biotechnology, Niihama National College of Technology, 7-1 Yagumo-cho, Niihama-shi 792-8580, Japan*

[e] *National Institute for Materials Science, 3-13 Sakura, Tsukuba, Ibaraki 305-0003, Japan*

[f] *CNRS, UPR3079 CEMHTI, 1D avenue de la Recherche Scientifique, 45071 Orléans cedex2, France*

*Corresponding author. Tel.: +81-3-5859-8150, fax +81-3-5859-8150

E-mail address: h-kioyono@sic.shibaura-it.ac.jp (H. Kiyono)

Abstract

We used magic angle spinning (MAS), multiquantum (MQ)-MAS, and high-temperature (HT) nuclear magnetic resonance (NMR) measurements to investigate the oxide-ion conduction path of oxygen-17 (O-17) in apatite-type lanthanum silicate $La_{9.33}(SiO_4)_6O_2$. A highly crystalline apatite-type lanthanum silicate was specifically synthesized for the measurements. MAS and MQ-MAS NMR confirmed that four kinds of oxide-ion sites are present in the structure and showed a small extra peak (<1%) possibly due to an interstitial site. The high-temperature measurements showed that the line shape changed and sharpened with increasing temperature from 200 ˚C, and the peak position shifted at 700 ˚C. The comparison of the results between MAS NMR (room-temperature) and HT static NMR showed the exchange of oxide ions bonded to Si (O1, O2, and O3) but the apparent exchange between the oxide ions (O1, O2, and O3) and the oxide ion at the isolated site (O4) is not observed. The exchange of the oxide ions that are bonded to Si (O1, O2, and O3) suggests that they are the main diffusion species in oxide-ion conductivity.

Key words: Apatite, Lanthanum Silicate, Oxide-ion conductor, Solid-state NMR, MQ MAS, High-temperature NMR

1. Introduction

Apatite-type Ln silicates, $Ln_{9.33+2x/3}(SiO_4)_6O_{2+x}$, (Ln: rare earth elements) and related materials are promising oxide-ion conductors and are used as electrolytes in high-temperature solid oxide fuel cells because of their high conductivity, which is comparable or superior to that of yttria-doped zirconia [1-7]. The high conductivity was first observed by one of the authors [1, 2]. Although the conduction mechanism has been extensively investigated [8-12], it has not been fully understood. Apatite has three kinds of sites for oxide ions in its structure (Fig. 1). Oxide ions (O1–O3) are located at the sites bonded to silicon and form SiO_4 tetrahedra, where O3 is assigned to two equivalent sites. On the contrary, the oxide ion labeled O4 is located in the center of the equatorial triangles of Ln1. Because the O4 site is located in the largest channel along the c-axis, the oxide ion at the O4 site seems to be the main migration specie [1]. In the study of single crystal Nd-Si-O apatite, the conductivity along the c-axis was found to be greater than that perpendicular to the c-axis; however, the difference between them decreases with increasing temperature, suggesting that the oxide ions migrate along the 001 direction. Furthermore, the migration perpendicular to the c-axis becomes significant at elevated temperatures [3, 5]. The maximum entropy method (MEM) has been used to fit the neutron diffraction patterns and to investigate the conduction mechanism. For

apatite-type $Ln_{9.33}(SiO_4)_6O_2$ (Ln = La, Nd) and $SrRe_8(SiO_4)_6O_2$ at room temperature, the

MEM results suggest that the oxide ion at the O4 site (as shown in Fig. 1) migrates

along the c-axis. The migration is induced by the slight rotation of the SiO_4 tetrahedra,

however, an apparent exchange between the oxide ions bonded to Si and O4 did not

occur. In addition, it was also reported that oxide ions located at the interstitial sites

were not observed in the samples [8]. Ali et al. performed MEM on Mg-doped

La-silicate $(La_{9.69}(Si_{5.70} Mg_{0.30})_{26.24})$ at room and high (1558 °C) temperature. They

showed that the oxide-ion migration is mainly caused by a vacancy mechanism in the

isolated (O4) oxide ion along the c-axis. However, the migration of oxide ion on

theO3-O5-O4 path is significant with increasing temperature, where O5 is the

interstitial oxide ion which is produced by the addition of MgO to La-apatite and is

present between O3 and O4 ions [9]. Computer simulations for oxygen-excess

$La_{9.67}(SiO_4)_6O_{2.5}$ apatite predicted that the presence of oxide ions at interstitial sites

near the SiO_4 tetrahedra form pseudo-"SiO_5" units[13, 14]. Oxide-ion conduction is

caused by a "hand-over" mechanism, where the interstitial oxide ion is transferred from

a SiO_4 unit to the next, momentarily forming a Si_2O_9 unit. A simulation study predicted

the presence of interstitial oxide ions but according to this study the ions located near

the O4 site diffuse along the c-axis via a vacancy diffusion mechanism [10]. Therefore

from our knowledge on the conduction mechanism in apatite, we observe that there are discrepancies in the presence and locations of the interstitial oxide ions.

To elucidate the oxide-ion conduction mechanism in apatite, we performed oxygen-17 (O-17) nuclear magnetic resonance (NMR) measurements. Among the apatite-type materials, we chose lanthanum silicate because of its high conductivity [1, 7]. O-17 NMR has been applied to investigate the structure around oxide ions [15] or defects in oxide-ion conductors [16-19]. It is well known that the line shape of the solid-state NMR spectrum is changed because of the motion that averages out anisotropic effecting terms such as chemical shift anisotropy, dipole-dipole, and quadrupole coupling effects. In addition, line shape of the solid-state NMR spectrum also changes with a fast site exchange. For species i, if more than two peaks are observed at different positions, δ_i, with intensity I_i at room temperature, then the nuclei at the sites are exchanged at a sufficiently higher rate as compared to the nuclear resonance frequency at elevated temperature. One apparent peak is observed at the weighted average, δ_{obs}, and is obtained using the following equation [20].

$\delta_{obs} = \Sigma\ \delta_i \cdot I_i /\ \Sigma I_i$ (1)

In a crystal possessing no structural changes at elevated temperature, the species concentration, which reflects the intensity (I_i), is proportional to the number of sites in

the crystal structure. Therefore, the comparison between the line shapes obtained at

room and elevated temperature give important information about the exchange of ions

among the sites because of the migration of oxide ions. In this study, oxygen-17 NMR

measurements were performed on La-Si-O silicate at room and high temperature to

elucidate the conduction mechanism of oxide ions in apatite-type La-silicate.

2. Experimental procedure

2.1 Preparation of La$_{9.33}$(SiO$_4$)$_6$O$_2$ apatite and O-17 enrichment

A sample of La$_{9.33}$(SiO$_4$)$_6$O$_2$ with high crystallinity was prepared for the O-17

measurements, because the typical powder process often results in the presence of

La$_2$SiO$_5$, which is difficult to eliminate during synthesis. La$_2$O$_3$ (99.9%) and SiO$_2$

(99.9%) powders were ball milled, dried, and calcined in air at 1200°C for 2 h. The

resulting La$_{9.33}$(SiO$_4$)$_6$O$_2$ powder was ball milled again to crush any agglomerations. The

fine La$_{9.33}$(SiO$_4$)$_6$O$_2$ powder was pressed to pellets and sintered at 1500 °C for 2 h in air.

The top surface of the sintered pellets was polished to be a mirror face, and a small

single seed crystal of La$_{9.33}$(SiO$_4$)$_6$O$_2$ specimen was bonded on the polished surface. The

seed crystal was grown using the Czochralski (Cz) method. The bonded sample was

heated at 1750 °C to change the polycrystalline region in the pellet to a crystalline

sample with large grains, because of grain growth at the interface between the seed

crystal and the pellet. The obtained sample was confirmed by X-ray diffraction (XRD,

Rigaku RINT-2000) and appeared as a single-phase ($La_{9.33}(SiO_4)_6O_2$) apatite with space

group $P6_{3/m}$. Furthermore, the crystalline sample was powdered by hand in a zirconia

mortar. To enrich the amount of O-17 in the sample, 0.3 g of the powdered sample was

heated in a platinum cell at 100, 200, 500, and 1000°C for 12 h in O-17-enriched water

vapor (40% O-17/O) at approximately 2 kPa [19].

2.2 Oxygen-17 NMR measurements

Oxygen -17 measurements were performed on a Bruker AVANCE-750 (17.5 T), -400

(9.3T), and JEOL ECA930 (21.9 T) spectrometer with a resonance frequency of 101.7,

54.2, and 126 MHz, respectively. We used the peak of $H_2{}^{17}O$ as a reference in the

abovementioned measurement. Magic-Angle Spinning (MAS) measurements at room

temperature were performed on AVANCE -400, -750, and ECA 930 at sample spinning

speeds of 14, 30, and 22 kHz, respectively. In the single-pulse MAS measurements, a

small angle excitation pulse ($\pi/18$ or $\pi/10$) was used to ensure the NMR intensity.

Multi-Quantum-MAS (MQ-MAS) measurements [21] were performed on an AVANCE

400 spectrometer. High-temperature (HT) measurements were also performed on

AVANCE 400 under static conditions. The sample was placed in the hexagonal boron

nitride container of the spectrometer. Both the top and the bottom surfaces of the container were heated by CO_2 lasers. The process of data acquisition started after the sample was heated at the desired temperature. Here, we do not describe the experimental details and the equipment used for the HT experiments [22, 23]. The obtained MAS, MQ-MAS, and HT static NMR spectra were analyzed using the DMFIT program [24].

3. Results and Discussion

3.1 O-17 MAS and MQ-MAS NMR spectra

Figure 2 shows the O-17 MAS NMR spectra of the samples at different heating temperatures during O-17 enrichment. The NMR measurements were performed at the room temperature. NMR signal was not detected in the sample that was enriched at 100 ˚C but the NMR signal was detected in the samples that were enriched at a temperature above 200 ˚C. Different signal-to-noise ratios are obtained due to different acquisition times. Each line shape consisted of one small (about 600 ppm) and two large (210 ppm and 190 ppm) peaks with a small shoulder (about 230 ppm). In addition, spinning side bands were also found. The line shape of each spectrum was almost the same but the value of the single to noise ratio varied. The similarity in the spectrum shows that the

heating temperature of the O-17 enrichment experiment above 200 ˚C does not affect

the line shape of the spectrum. In the NMR measurements, we used the sample

enriched at 1000 ˚C for 12 h.

Figure 3 shows the MQ-MAS spectrum at approximately 180 ppm. Broadening in

the MAS dimension is caused by the distribution in the chemical shift (CS) and

quadrupolar coupling constants (QCC), however, broadening in the isotropic dimension

is mainly caused by the distribution in the chemical shift. The contours of the

experimental spectrum broaden diagonally (Fig. 3(a)), showing that the distribution in

both CS and QCC is present in the peaks at approximately 180 ppm. The observed

spectrum was simulated with the DMFIT program, taking into account of the Gaussian

distribution in CS and QCC for each peak. The simulated contours are shown in Fig.

3(b) and the parameters obtained by the simulation are listed in Table 1. If three peaks

in the simulation results in good agreement with the observations, then we can suggest

that the peak observed in Fig. 3(a) consists of more than three components.

Figure 4 shows the MAS NMR spectrum of the sample obtained by using

AVANCE–750 with the simulated line shape. A simulated line was also obtained by

using the DMFIT program. In the simulation, the CS, QCC, and their distributions for

the three components, #1 to #3, were fixed at the values obtained by the analysis of the

MQ MAS measurements. For the other components, #4 to #6, the parameters were obtained by fitting the observations with a Gaussian function because the peaks had a simple symmetrical shape. All except the fixed parameters of the components, which were obtained by the analysis of the MQ MAS result, were optimized by a least- square method. When the presence of six components was assumed, the observed line shape was well represented by the simulated line shape, as shown in Fig. 4. The obtained parameters were also listed in Table 1.

3.2 Assignment of the peaks

The presence of four peaks suggests that four kinds of oxygen sites are present in the structure because it is reported that the oxygen bonded to Si is commonly found at approximately 200 ppm [25]. It is reasonable to assign the peaks to the O1 to O3 sites, which represents the sites where the oxide ions are bonded to the silicon. The ratio of the intensity of the peaks at #1 (165 ppm), #2 (194 ppm), and #3 (214 ppm) to the intensity obtained by the simulation (Table 1) is calculated to be 22:55:23. This ratio shows good agreement with the stoichiometric value of 1:2:1 corresponding to O1:O3:O2. This agreement suggests that the peaks of #1, #2, and #3 are O1 (or O2), O3, and O2 (or O1), respectively. It is impossible to assign O1 and O2 to #1 and #3 individually, based on only the intensity ratio of the peaks. The intensity ratio of peak #4 at 600 ppm is

7.7% The intensity ratio of #4 to the sum of #1–#4 is about 8.1%, which is in good agreement with the calculated value of 7.6% for the O4 site that is based on the stoichiometry of the apatite. The oxide ion in lanthanum oxide-related materials was found in the range 450–600 ppm [26]. Therefore, the peak of #4 at 600 ppm could be assigned to the O4 site, as shown in Fig. 1. The peak of #5 has an intensity ratio of 0.8%. It is impossible to estimate small intensity ratios that are based on the stoichiometry and crystal structure of apatite. This peak suggests the presence of interstitial site oxygen. Because the oxygen atoms bonded to silicon in silicate materials is usually found to be approximately 200 ppm [25], the interstitial oxide ion is inferred to be near the silicon atom in the structure. However, the peak is too small to be confirmed and hence requires further research. A peak at approximately 400 ppm (#6) is seen in the spectrum. In a previous report on O-17 NMR study in silicates, and lanthanum oxide and related materials, no peak at approximately 400 ppm was reported. On the contrary, it was reported that the peaks of oxide ions in zirconia and zirconia-based materials are typically found at approximately 400 ppm [25]. Therefore, the peak at 400 ppm is believed to be due to contamination of zirconia-related materials, which are incorporated during the crushing process of the apatite sample by the ZrO_2 motor. Traces of Zr were also detected by the X-ray fluorescence analysis in the powdered

sample. Because ZrO_2 does not react with apatite at 1000 ˚C, which is the temperature

during O-17 enrichment process, it was assumed that the effect of contamination was

negligible.

3.3 HT NMR spectra

Figure 5 shows the in situ HT static NMR spectra, in which the intensity of the

spectrum is scaled to the signal intensity except for the one obtained by the MAS

experiments (Fig. 5 (a)). At room temperature, the spectrum obtained by the static

experiments (Fig. 5 (b)) was broader than and shifted from that by the MAS

experiments. It is known in NMR of quadrupolar nuclei such as O-17 that a shape and

position of MAS spectrum changes from that of static spectrum [27]. Therefore the

static spectrum was apparently shifted from that of MAS spectrum. The peak at

approximately 600 ppm could not be distinguished in the spectrum obtained by the

static condition because the peak becomes broader and sufficient signal to noise ratio is

not achieved in the static condition. The peak intensity of the spectrum decreased in

accordance with the increasing temperature (300–500 ˚C). At 600 ˚C, the intensity and

width became greater and narrower, respectively. At 700 ˚C, the peak became narrow

and was observed at approximately 190 ppm. It was confirmed that the peak was not

observed at approximately 600 ppm, even when the observed area around 600 ppm

shifted due to a change in the irradiating pulse frequency. The abovementioned occurred because the peak was too small to be distinguished from the noise.

The spectrum of each temperature was simulated by one Gaussian-shaped peak and the peak positions were obtained, which are plotted in Fig. 6 against the heating temperature with two calculated peak positions. The peak positions were able to be calculated by using equation (1) based on the following two assumptions. First, a value of 191.6 ppm is obtained by assuming that the sites O1, O2, and O3 exchanged among themselves, whereas site O4 did not exchange with the others. This assumption corresponds to the notion that the O4 diffusion is independent of the oxide ions at O1–O3. Second, the value of 224.4 ppm is obtained by assuming that the sites O1, O2, O3, and O4 are equally exchanged. This assumption corresponds to the condition that all oxygen sites (O1~O4) exchange among themselves. In the both assumptions, the data of O5 was ignored, because the intensity of O5 was too small to affect the calculated values significantly. The two calculated values were also shown in Fig. 6 by the two horizontal dashed lines. The observed peak position above 700 ˚C is at 186.4 ppm and this value is in good agreement with the calculated value of 191.6 ppm, which is based on the former assumption. This agreement shows that fast exchange among the O1, O2, and O3 sites occurs at 700 ˚C. If the exchange of oxide ions occurs within one

SiO$_4$ tetrahedra, then the oxide ions would move only in the tetrahedra, corresponding to a rotation of SiO$_4$ unit, and oxide-ion conductivity in the macro scale would not be observed. However, oxide-ion conductivity is observed at 700 °C in apatite with the same composition with this material [7] showing that oxide ions migrate in the bulk scale. Therefore, the SiO$_4$ tetrahedra can exchange oxide ions and the oxide ions of O1, O2 and O3 are the main migration species in the apatite and such exchange facilitates bulk oxide-ion migration. This conduction mechanism of oxide ions agrees with the proposed model stating that conduction is facilitated by the exchange of oxide ions between neighboring SiO$_4$ units [13, 28]. Movement of oxide ion at the O4 site could not be detected in this study. To elucidate the movement of oxide ions at the O4 site, further investigations to obtain spectra with high signal to noise ratio and higher temperature experiments are needed.

4. Conclusions

Oxygen-17 MAS, MQ-MAS, and HT static NMR measurements were performed on apatite-type lanthanum silicate, La$_{9.33}$(SiO$_4$)$_6$O$_2$. Highly crystalline apatite was synthesized for the NMR experiments. In the MQ-MAS and MAS NMR experiments, the obtained spectrum was analyzed, and the oxygen sites were assigned to the

convoluted peaks that are based on previous reports and stoichiometry. Peaks at

approximately 200 ppm were assigned to the oxide ions bonded to the Si atom, and the

small peak at approximately 600 ppm was assigned to the oxide ion at the site

surrounded by La. In addition, one small peak was observed (<1%), which was not

assigned on the basis of the crystal structure, suggesting the presence of interstitial

oxide ions. In HT static NMR measurements, spectra were obtained at a temperature

up to 700°C. A broad peak observed at the room temperature was located at

approximately 140 ppm, which decreased with increasing temperature, up to 500 °C.

The peak position was gradually shifted to 186 ppm with increasing the temperature

from 400 to 600 °C. The peak became sharp and further increased up to 600°C. At 700°C,

the spectrum shows one sharp peak at 186 ppm. This shift of the peak at 700 °C could be

explained via a process of fast exchange among the oxide ions at O1, O2, and O3. This

exchange suggests that O1, O2, and O3 are the main migration species and the

conduction of oxide ions is caused by a handover mechanism between neighboring SiO_4

units.

Acknowledgments

References

 [1] S. Nakayama, T. Kageyama, H. Aono and Y. Sadaoka, J. Mater. Chem., 5 (1995) 1801.

 [2] S. Nakayama and M. Sakamoto, J. Eur. Ceram. Soc., 18 (1998)1413.

 [3] S. Nakayama, M. Sakamoto, M. Higuchi, K. Kodaira, M. Sato, S. Kakita, T. Suzuki and K. Itoh, J. Eur. Ceram. Soc., 19 (1999)507.

 [4] M. Higuchi, K. Kodaira and S. Nakayama, J. Cryst. Growth, 207 (1999)298.

 [5] M. Higuchi, Y. Masubuchi, S. Nakayama, S. Kikkawa and K. Kodaira, Solid State Ionics 174 (2004) 73.

 [6] H. Yoshioka and Y. Nojiri, S. Tanase, Solid State Ionics, 179 (2008) 2165.

 [7] Y. Higuchi, M. Sugawara, K. Onishi, M. Sakamoto and S. Nakayama, Ceram. Int., 36 (2010) 955.

 [8] Y. Masubuchi, M. Higuchi, T. Takeda and S. Kikkawa, Solid State Ionics, 177 (2006) 263.

 [9] R. Ali, M. Yashima, Y. Matsushita, H. Yoshioka, K. Ohoyama and F. Izumi, Chem. Mater., 20 (2008) 5203.

 [10] E. Bechade, O. Masson, T. Iwata, I. Julien, K. Fukuda, P. Thomas and E. Champion, Chem. Mater., 2 (2009) 2508.

 [11] V. V. Kharton, A. L. Shaula, M. V. Patrakeev, J. C. Waerenborgh, D. P. Rojas, N. P. Vyshatko, E. V. Tsipis, A. A. Yaremchenko and F. M. B. Marques, J. Electrochem. Soc., 151 (2004) A1236.

 [12] E. Kendrick, M. S. Islam and P. R. Slater, Chem. Commun., 6 (2008)715.

 [13] A. Jones, P. R. Slater and M. S. Islam, Chem., Mater., 20 (2008)5055.

 [14] E. Kendrick, M. S. Islam and P. R. Slater, J. Mater. Chem., 17 (2007) 3104.

 [15] H. Maekawa, P. Florian, D. Massiot, H. Kiyono and M. Nakamura, J. Phys. Chem., 100 (1996) 5525.

 [16] N. Kim, C. H. Hsieh, H. Huang, F. B. Prinz and J. F. Stebbins, Solid State Ionics, 178 (2007) 1499.

 [17] L. M. Peng and J. F. Stebbins J. Non-Cryst. Solids, 354 (2008) 3120.

 [18] J. F. Stebbins, E. V. Dubinsky, K. Kanehashi and K. E. Kelsey, Geochimica Et Cosmochimica Acta 72 (2008) 910.

 [19] M. Ando, I. Oikawa, Y. Noda, S. Ohki, M. Tansho, T. Shimizu, H. Kiyono and H. Maekawa, Solid State Ionics, 192 (2011) 576.

 [20] M. H. Levitt, Spin Dynamics -Basics of Nuclear Magnetic Resonance-, 1st ed., WILEY & SONS: Chichester, (2001), p495.

 [21] D. Massiot, J. Magn. Reson. Ser A, 122 (1996)240.

[22] R. Winter, A. Jones, R. Shaw-West, M. Wolff, P. Florian and D. Massiot, Appl. Magn. Reson., 32 (2007) 635.

[23] B. T. Poe, P. F. Mcmillan, B. Cote, D. Massiot and J. P. Coutures, J. Amer. Ceram. Soc., 77 (1994) 1832.

[24] D. Massiot, F. Fayon, M. Capron, I. King, S. Le Calve, B. Alonso, J. O. Durand, B. Bujoli, Z. H. Gan and G. Hoatson, Magn. Reson. Chem., 40 (2002) 70.

[25] K. J. D. MacKenzie and M. E. Smith, Multinuclear Solid-State Nuclear Magnetic Resonance of Inorganic Materials, Pergamon Press, 2002, p362.

[26] T. J. Bastow, P. J. Dirken, M. E. Smith and H. J. Whitfield, J. Phys. Chem., 100 (1996) 18539.

[27] D. Freude, In: R.A. Meyers, Editor, *Encyclopedia of Analytical Chemistry*, John Wiley & Sons Ltd, Chichester (2000), 12188.

[28] J. E. H. Sansom, J. R. Tolchard, M. S. Islam, D. Apperley and P. R. Slater, J. Mater. Chem., 16 (2006) 1410.

Figure captions

Fig. 1 Crystal structure of apatite-type rare earth silicate viewed along the c-axis.

Fig. 2 O-17 MAS NMR spectra of the $La_{9.33}(SiO_4)_6O_2$ measured by ECA930. The enrichment of O-17 was performed at (a) 200 ˚C, (b) 300 ˚C, and (c) 1000 ˚C for 12 h. The black circle denotes the spinning side bands. Because the number of acquisition times was different in the samples, the signal to noise ratio of the spectra does not directly reflect the concentration of oxygen-17 in the samples.

Fig. 3 (a) Observed MQ-MAS NMR spectra of the $La_{9.33}(SiO_4)_6O_2$ sample measured on AVANCE-400 and (b) simulated MQ-MAS NMR spectra.

Fig. 4 MAS NMR spectrum of the $La_{9.33}(SiO_4)_6O_2$ sample measured by AVANCE-700 with the simulated line shape. The simulated spectrum is the sum of the peaks of the components and spinning side bands (S.S.B.). Asterisks denote the peak possibly due to ZrO_2 contamination during powdering of the apatite.

Fig. 5 High-temperature O-17 static and MAS NMR spectra of the $La_{9.33}(SiO_4)_6O_2$ sample measured by AVANCE-400 with (a) MAS NMR spectrum at room temperature for comparison. Spectra were obtained at (b) room temperature, (c) 200˚C, (d) 300˚C, (e) 400 ˚C, (f) 500 ºC, (g) 600 ˚C, and (h) 700 ˚C.

Fig. 6 Plots of the values of the chemical shift of the peaks shown in Fig. 5 against temperature. The values of the chemical shift were obtained by fitting a Gaussian function to the observed line shape. Upper and lower dashed lines denotes the calculated values obtained by the assumptions of the site exchange among all oxide ions sites and among the O1, O2, and O3 sites, respectively.

Table 1 O-17 MQ-MAS and MAS NMR fitting parameters obtained for $La_{9.33}(SiO_4)_6O_2$. Values in italic are the fixed parameters in the fitting.

	#1						#2						#3						#4			#5			#6		
	I	δ_{iso}	$\Delta\delta_{iso}$	nQ	ΔnQ	η	I	δ_{iso}	$\Delta\delta_{iso}$	nQ	ΔnQ	η	I	δ_{iso}	$\Delta\delta_{iso}$	nQ	ΔnQ	η	I	δ_{iso}	$\Delta\nu_{1/2}$	I	δ_{iso}	$\Delta\nu_{1/2}$	I	δ_{iso}	$\Delta\nu_{1/2}$
MQ-MAS	27.1	165	14	266	150	0.6	66.2	194	31	264	150	0.6	6.7	214	71	305	150	0.6									
MAS	19.8	*165*	*14*	*266*	*150*	*0.6*	48.1	*194*	*31*	*264*	*150*	*0.6*	19.2	*214*	*71*	*305*	*150*	*0.6*	7.7	600	2.6	0.8	241	2.2	4.4	380	2.1

I, Intensity (%)

δ_{iso}, Isotropic Chemical Shift (ppm)
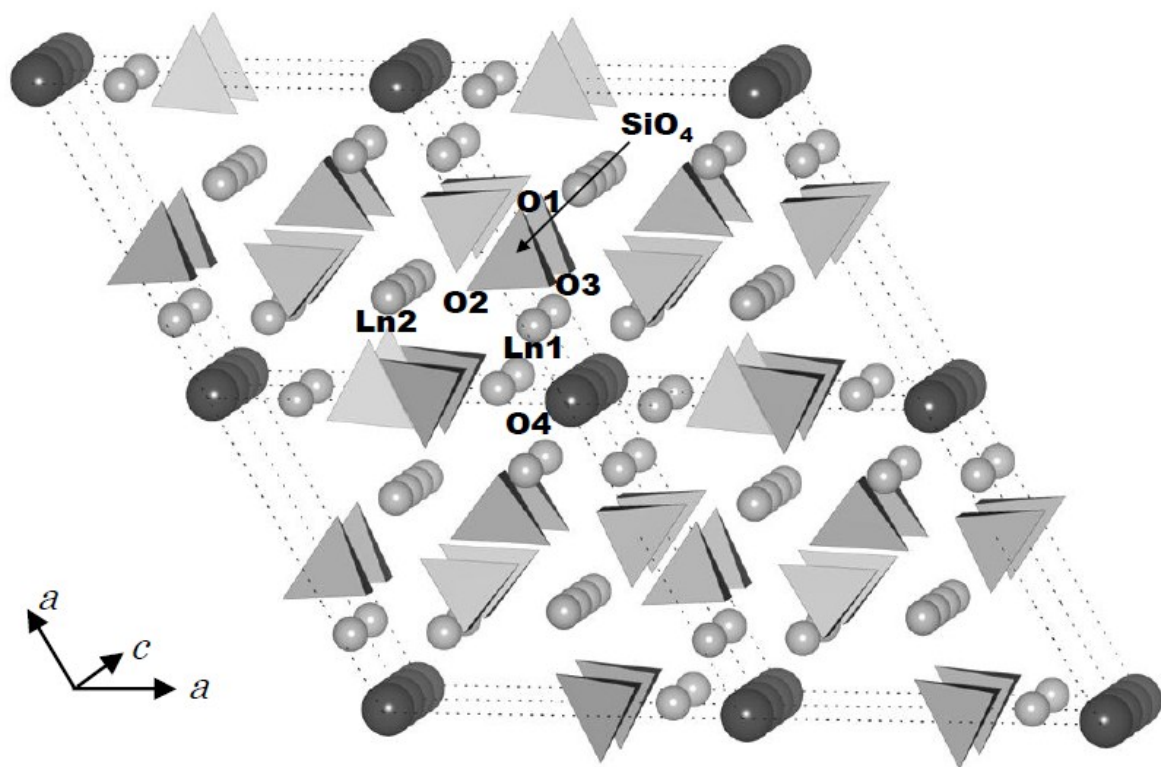
$\Delta\delta_{iso}$, Distribution of δ_{iso} (ppm)
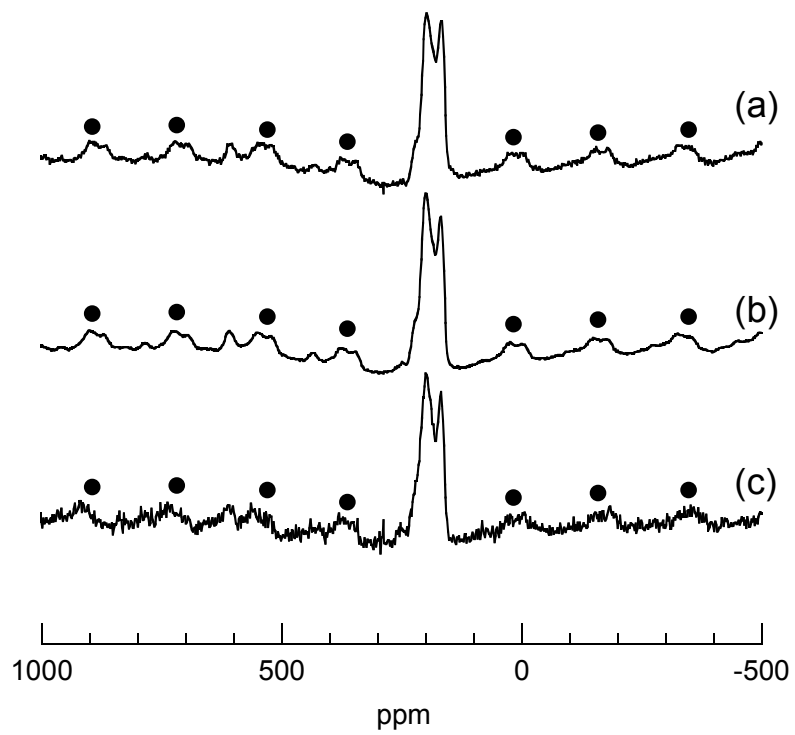
nQ, Nuclear Quadrupolar Coupling Constants (kHz)

ΔnQ, Distribution of *nQ* (kHz)

η, Asymmetry parameter for *nQ*

$\Delta\nu_{1/2}$, Half width at half high

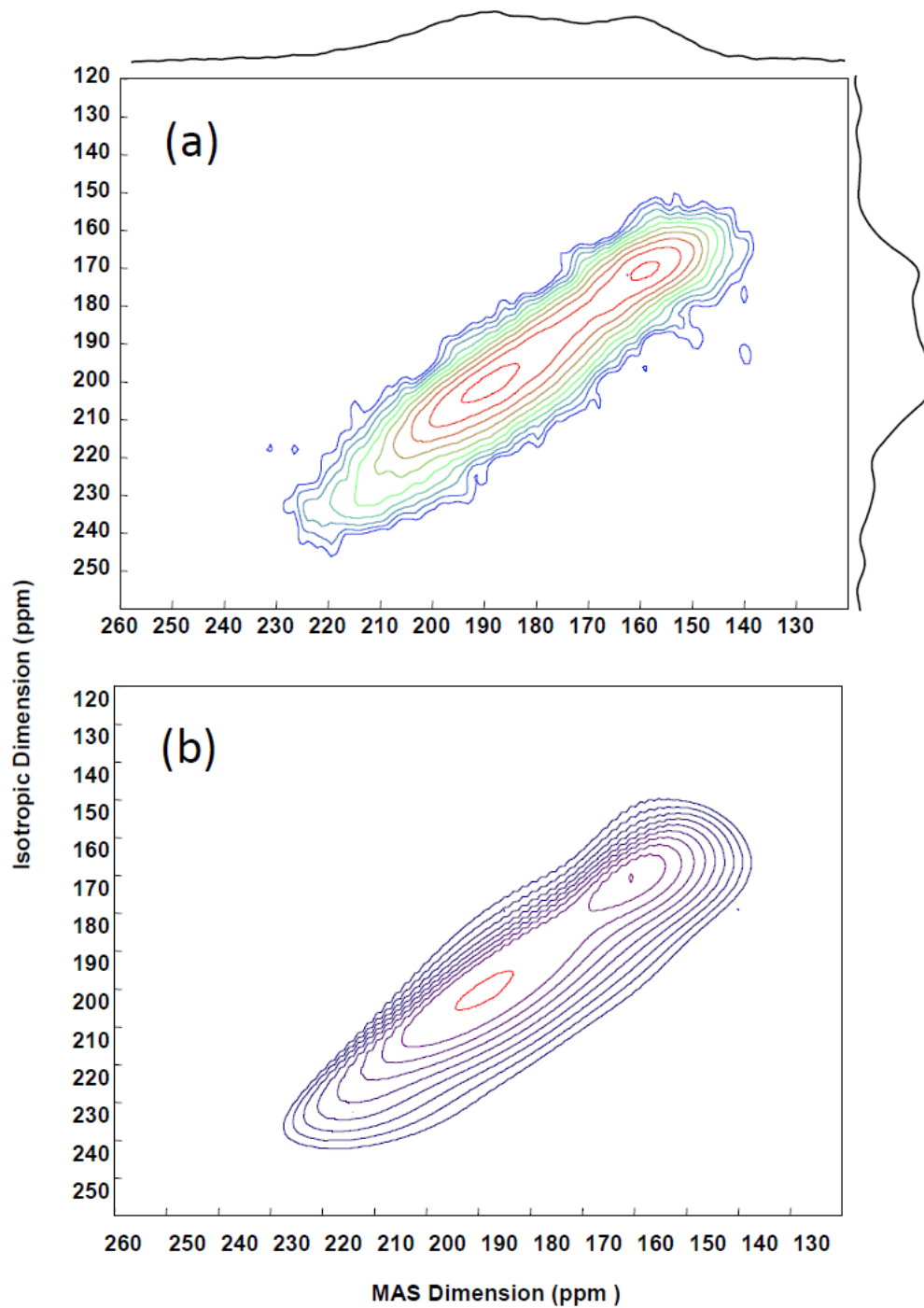H. Kiyono et al   Fig. 1

(a)
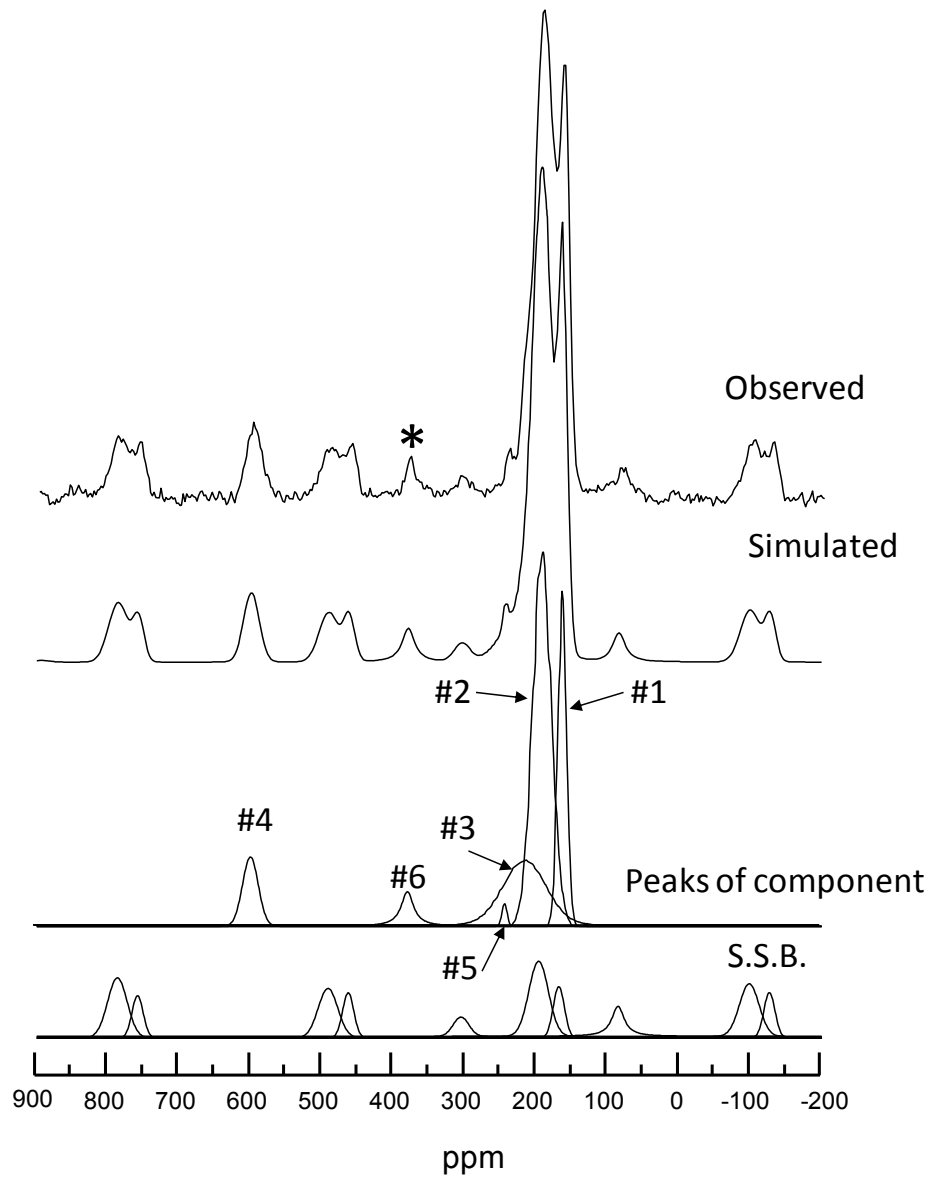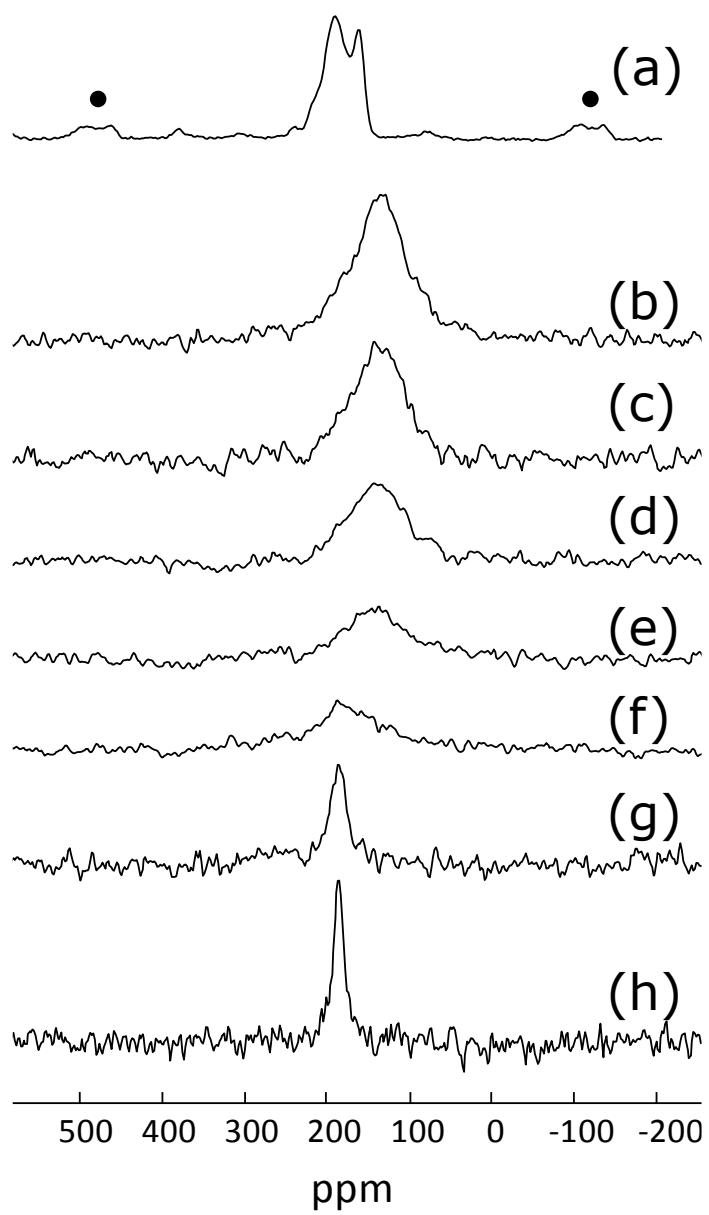
(b)

(c)

1000   500   0   -500

ppm

H. Kiyono et al   Fig. 2

H. Kiyono et al   Fig. 3

Observed

Simulated

#2 → #1

#4

#3

#6

Peaks of component

#5

S.S.B.

900 800 700 600 500 400 300 200 100 0 -100 -200

ppm

H. Kiyono et al   Fig. 4

25

500 400 300 200 100 0 -100 -200

ppm

H. Kiyono et al   Fig. 6